Acta Crystallographica Section D
Biological Crystallography
ISSN 0907-4449

The structure of human phosphoglucose isomerase complexed with a transition-state analogue

Christopher Davies,[a]* Hilary Muirhead[b] and John Chirgwin[c]

[a]Department of Biochemistry and Molecular Biology, Medical University of South Carolina, Charleston, SC 29425, USA, [b]School of Medical Sciences, University of Bristol, Bristol BS8 1TD, England, and [c]Department of Medicine, University of Virginia, Charlottesville, VA 22908, USA

Correspondence e-mail: davies@musc.edu

Phosphoglucose isomerase (PGI) is a workhorse enzyme of carbohydrate metabolism that interconverts glucose 6-phosphate and fructose 6-phosphate. Outside the cell, however, the protein appears to function as a cytokine. A crystal structure of human PGI bound with 5-phosphoarabinonate, a strong inhibitor that mimics the *cis*-enediol(ate) intermediate of the reaction, has been determined at 2.5 Å resolution. The structure helps to confirm the assignment of Glu357 as the base catalyst in the isomerase reaction.

Received 19 February 2003
Accepted 1 April 2003

PDB Reference: phosphoglucose isomerase–5-phosphoarabinonate, 1nuh, r1nuhsf.

1. Introduction

Phosphoglucose isomerase (EC 5.3.1.9) is a workhorse enzyme of sugar metabolism. It catalyses the second step of glycolysis, the interconversion of glucose 6-phosphate (G6P) and fructose 6-phosphate (F6P), by transfer of a proton between the C2 position of G6P and C1 of F6P (Rose, 1975). Recent crystal structures of the enzyme have led to proposals that Glu357 is the active-site base responsible for this transfer (Lee *et al.*, 2001; Read *et al.*, 2001) and that either His388 or Lys518 catalyses the ring-opening of the sugar substrate (Davies & Muirhead, 2003; Lee *et al.*, 2001). The human enzyme is of medical interest because mutations in this enzyme lead to non-spherocytic haemolytic anaemia (Baughan *et al.*, 1968) and because high levels of PGI activity are measured in the sera of patients with certain cancers (Baumann *et al.*, 1990).

Interest in PGI has grown following the discoveries that it manifests cytokine function in a wide variety of cellular activities (Gurney *et al.*, 1986; Watanabe *et al.*, 1996; Xu *et al.*, 1996) and appears to be an antigen in rheumatoid arthritis (Matsumoto *et al.*, 1999) and sperm agglutination (Yakirevich & Naot, 2000). To what extent the enzymatic properties of PGI overlap with its cytokine functions remains unclear.

Here, we present the crystal structure of human PGI bound to a transition-state analogue, 5-phosphoarabinonate (PAB), solved at 2.5 Å resolution. Along with equivalent structures obtained from pig and rabbit sources (Davies & Muirhead, 2002; Jeffery *et al.*, 2001), it supports the hypothesis that Glu357 is the base catalyst in the reaction mechanism.

2. Experimental

Human PGI was purified and crystallized as described previously (Read *et al.*, 2001) except that 5 m*M* PAB was included in the protein drops. The resulting crystals were of the same morphology as native crystals but diffracted X-rays less well. After stabilization in a solution containing 2.1 *M* ammonium sulfate, 100 m*M* Tris–HCl pH 8.5 and 30% glycerol, the crystals were flash-frozen to 100 K. Data were collected with an R-AXIS IV^{++} detector positioned at a crystal-to-detector distance of 160 mm and mounted on an RU3-HBR X-ray generator (Rigaku-MSC) fitted with Osmic mirror optics. The crystals belonged to space group $P4_32_12$, with unit-cell parameters $a = b = 94.4$, $c = 137.1$ Å. A total of 173 frames were collected in 0.5° oscillations to ensure high redundancy, with an exposure time of 5 min per frame. The data were processed using *d*TREK* (Pflugrath, 1999). The starting model for refinement was the 1.6 Å resolution structure of human PGI (Read *et al.*, 2001) from which a bound sulfate and all waters molecules had been removed. After initial refinement using *X-PLOR* (Brünger, 1992), both $2(|F_o| - |F_c|)$ and $(|F_o| - |F_c|)$ electron-density maps clearly showed the PAB molecule bound at the active site. After a molecule PAB was fitted to the density, subsequent rounds of refinement used *REFMAC* (Murshudov *et al.*, 1997). The final model is numbered 1–555 and includes one PAB molecule, six sulfate mole-

Table 1
X-ray diffraction data and refinement statistics.

Values in parentheses are for the outer resolution shell.

Data collection	
Resolution range (Å)	50–2.5 (2.59–2.5)
R_{merge}† (%)	12.8 (25.4)
Redundancy	6.9 (6.8)
Completeness (%)	98.4 (99.8)
$\langle I\rangle/\langle\sigma(I)\rangle$	5.7 (3.1)
Refinement	
Resolution range (Å)	50.0–2.5
σ cutoff applied	0.0
Total No. of reflections	21468
Reflections used in R_{free} (%)	5.0
No. of non-H protein atoms	4424
No. of sulfate molecules	6
No. of water molecules	109
R factor (%)	21.7
R_{work} (%)	21.4
R_{free} (%)	26.8
R.m.s. deviations from ideal stereochemistry	
Bond lengths (Å)	0.011
Bond angles (°)	1.48
B factors (Å^2)	
Overall B factor	25.16
Mean B factor (main chain)	24.55
R.m.s. deviation in main-chain B factor	0.390
Mean B factor (side chains and waters)	25.72
R.m.s. deviation in side-chain B factors	1.454
Ramachandran plot statistics (%)	
Residues in most favoured region	88.8
Residues in additionally allowed regions	10.8
Residues in generously allowed regions	0.4
Residues in disallowed regions	0.0

† $R_{merge} = \sum|I_i - I_m|/\sum I_i$, where I_i is the intensity of the measured reflection and I_m is the mean intensity of all symmetry-related reflections.

cules (arising from the crystallization solution) and 109 water molecules. The data-collection and refinement statistics are shown in Table 1.

3. Results and discussion

3.1. Structure description

PGI has been solved from a variety of mammalian sources and from *Bacillus stearothermophilus* in both native and inhibitor-bound forms (see, for example, Davies & Muirhead, 2002; Jeffery *et al.*, 2000; Read *et al.*, 2001; Sun *et al.*, 1999). The protein architecture is essentially identical in mammalian PGIs and is highly similar in the enzyme from *B. stearothermophilus*. The structure comprises two domains, termed large and small, where each domain consists of a central β-sheet surrounded by α-helices. The active site is located in a crevice between the large and small domains, near the subunit boundary. The enzyme form of human PGI exists as a dimer (Tilley *et al.*, 1974), but since it crystallizes as a monomer in the asymmetric unit a symmetry operation is required to generate the dimer. The active site comprises residues that are likely to play a role in the catalytic mechanism, including Glu357, Arg272, His388 and Lys518. One of these residues, His388, is contributed by the adjacent monomer.

3.2. Ligand binding

PAB is a competitive inhibitor of PGI that is believed to mimic the *cis*-enediolate intermediate of the catalytic reaction (Chirgwin & Noltmann, 1975). Our structure of human PGI in complex with PAB helps to further resolve the ambiguity regarding the binding mode of this inhibitor. The PAB molecule is bound to the active site in essentially an identical manner to that seen in equivalent complexes of PGI from rabbit (Jeffery *et al.*, 2001) and pig (Davies & Muirhead, 2002), but the opposite of that seen in a complex with PGI from *B. stearothermophilus* (Chou *et al.*, 2000) (Fig. 1). As expected, the sulfate molecule that was observed in the active site of the native structure (Read *et al.*, 2001) has been displaced by the phosphate group of the PAB inhibitor. The phosphate group is oriented by the same cluster of serine and threonine side chains (Ser209, Thr211, Thr214 and Ser159) as well as the amide N atoms of Lys210 and Thr211 and by one water molecule to Thr217. Both the C2 and C3 hydroxyls (equivalent to C3 and C4 of the substrate) are within hydrogen-bonding distance of the amide group of Gly158. This region of the inhibitor lies close to the turn formed by Gly157 and Gly158 and the absence of side chains in these positions facilitates a closer binding of the substrate. The monitoring of these two hydroxyls by Gly158 probably contributes to the high specificity of PGI for its sugar substrates. One of the side-chain O atoms of Glu357 lies close to O1A and C1 of PAB as well as to the guanidinium group of Arg272. This arrangement suggests that Glu357 is best placed to abstract a proton from the C2 and C1 positions of G6P and F6P, respectively, as proposed recently (Lee *et al.*, 2001; Read *et al.*, 2001), and that the positive charge of Arg272 may stabilize the negative charge of the *cis*-enediolate intermediate. Lys518 and His388 both contact O4, which is equivalent to the ring oxygen of the substrate, and Lys518 also contacts O5. Either or both of these residues may participate in ring opening.

3.3. Comparison with native human PGI

Two structures of human PGI have been published. The first of these contains a sulfate in the active site that appears to mimic the phosphate moiety of the substrate (Read *et al.*, 2001), whereas the second structure is free of ligands and so better represents the true native state of the enzyme (Tanaka *et al.*, 2002). Comparisons of the sulfate-bound structure with a ligand-free structure of rabbit PGI suggested that elements of the small domain shift from an 'open' to 'closed' conformation upon binding sulfate (Read *et al.*, 2001). The hypothesis that the sulfate moiety was mimicking the sugar phosphate is confirmed by the human PAB-bound structure, in which the same region of the small domain is seen in the 'closed' conformation. In contrast, all four molecules present in the

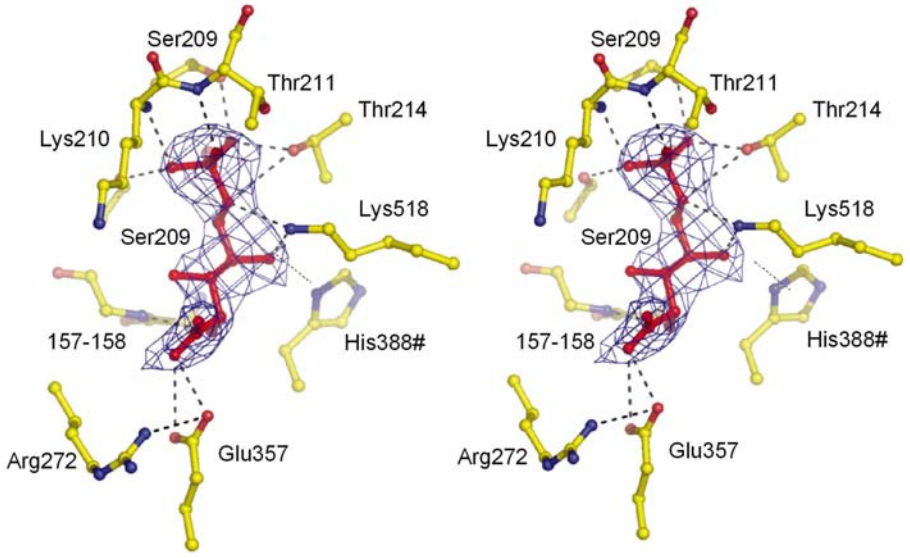

Figure 1
5-Phosphoarabinonate bound to human phosphoglucose isomerase at 2.5 Å resolution. A stereo picture of the active-site region, showing the $2(|F_o| - |F_c|)$ electron density of the bound inhibitor, contoured in blue at 1σ. The active-site residues and inhibitor molecules are shown in ball-and-stick form. The inhibitor is coloured red. This figure was prepared using *PyMOL* (DeLano, 2002).

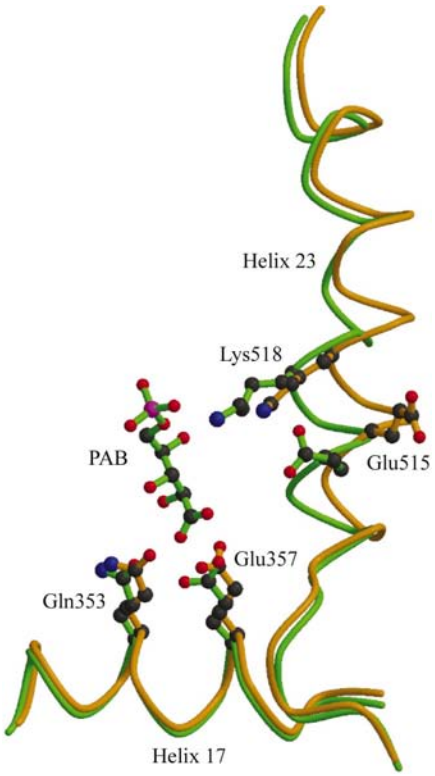

Figure 2
The shift of α23 caused by the binding of 5-phosphoarabinonate. Shown is a backbone superimposition of the sulfate-bound human structure (Read *et al.*, 2001) coloured in orange and the PAB-bound structure in green. Important residues are shown in ball-and-stick representation, in which the bonds are coloured the same as the backbone. Note the rotation of the carboxylate of Glu357 and the slight shift of the adjacent residue, Gln353. For clarity, only helices 23 and 17 are shown. This figure was prepared using *MOLSCRIPT* (Kraulis, 1991).

structure of a ligand-free human PGI are seen in the 'open' conformation (Tanaka *et al.*, 2002).

The only other structural difference of significance is the shift of the N-terminal half of helix α23 (residues 512–520) toward the active site which occurs in the PAB-bound structure but in neither of the human native structures (Fig. 2). The same movement of α23 has been seen in the pig and rabbit homologues of PGI (Arsenieva & Jeffery, 2002; Davies & Muirhead, 2002, 2003). The shift of Lys518 toward the active site and its close proximity to the ring oxygen is concordant with a role for this residue in ring opening. Interestingly, the carboxylate group of Glu357 rotates by approximately 90° to align more closely with the carboxylate on the PAB molecule. In the case of the true substrate, a similar repositioning would enhance the ability of Glu357 to abstract a proton from the C1/C2 positions (Fig. 2).

4. Conclusion

The structure of human PGI bound to 5-phosphoarabinonate further establishes Glu357 as the best candidate for base catalyst, as proposed recently (Lee *et al.*, 2001; Read *et al.*, 2001), supplanting earlier suggestions that His388 was responsible (Chou *et al.*, 2000; Jeffery *et al.*, 2000). Instead, His388 is likely to be the acid catalyst for ring opening. The close proximity of Lys518 to the ring oxygen and its shift towards the active site upon PAB binding suggest that it too has a role in the mechanism of ring opening. PGI is becoming increasingly better characterized as an enzyme, but much remains to be elucidated regarding its cytokine function.

The authors wish to thank Klaus Schnackerz for the kind gift of the 5-phosphoarabinonate used in this study. This research was supported by grants from the US Army (DAMD17-98-1-8245 and DAMD17-02-1-0586) to JMC.

References

Arsenieva, D. & Jeffery, C. (2002). *J. Mol. Biol.* **323**, 77–84.
Baumann, M., Kappl, A., Lang, T., Brand, K., Siegfried, W. & Paterok, E. (1990). *Cancer Invest.* **8**, 351–356.
Baughan, M. A., Valentine, W. N., Paglia, D. E., Ways, P. O., Simons, E. R. & DeMarsh, Q. B. (1968). *Blood*, **32**, 236–249.
Brünger, A. T. (1992). *X-PLOR. Version 3.1. A System for X-ray Crystallography and NMR.* Yale University, New Haven, CT, USA.
Chirgwin, J. M. & Noltmann, E. A. (1975). *J. Biol. Chem.* **250**, 7272–7276.
Chou, C.-C., Sun, Y.-J., Meng, M. & Hsiao, C.-D. (2000). *J. Biol. Chem.* **275**, 23154–23160.
Davies, C. & Muirhead, H. (2002). *Proteins Struct. Funct. Genet.* **49**, 577–579.
Davies, C. & Muirhead, H. (2003). *Acta Cryst.* D**59**, 453–465.
DeLano, W. L. (2002). *The PyMOL Molecular Graphics System*, http://pymol.sourceforge.net.
Gurney, M. E., Apatoff, B. R., Spear, G. T., Baumel, M. J., Antel, J. P., Bania, M. B. & Reder, A. T. (1986). *Science*, **234**, 574–581.
Jeffery, C. J., Bahnson, B. J., Chien, W., Ringe, D. & Petsko, G. A. (2000). *Biochemistry*, **39**, 955–964.
Jeffery, C. J., Hardre, R. & Salmon, L. (2001). *Biochemistry*, **40**, 1560–1566.
Kraulis, P. J. (1991). *J. Appl. Cryst.* **24**, 946–950.
Lee, J. H., Chang, K. Z., Patel, V. & Jeffery, C. J. (2001). *Biochemistry*, **40**, 7799–7805.
Matsumoto, I., Staub, A., Benoist, C. & Mathis, D. (1999). *Science*, **286**, 1732–1735.
Murshudov, G. N., Vagin, A. A. & Dodson, E. J. (1997). *Acta Cryst.* D**53**, 240–255.
Pflugrath, J. W. (1999). *Acta Cryst.* D**55**, 1718–1725.
Read, J., Pearce, J., Li, X., Muirhead, H., Chirgwin, J. & Davies, C. (2001). *J. Mol. Biol.* **309**, 447–464.
Rose, I. A. (1975). *Adv. Enzymol. Relat. Areas Mol. Biol.* **43**, 491–517.
Sun, Y. J., Chou, C. C., Chen, W. S., Wu, R. T., Meng, M. & Hsiao, C. D. (1999). *Proc. Natl Acad. Sci. USA*, **96**, 5412–5417.
Tanaka, N., Haga, A., Uemura, H., Akiyama, H., Funasaka, T., Nagase, H., Raz, A. & Nakamura, K. (2002). *J. Mol. Biol.* **318**, 985–997.
Tilley, B. E., Gracy, R. W. & Welch, S. G. (1974). *J. Biol. Chem.* **249**, 4571–4579.
Watanabe, H., Takehana, K., Date, M., Shinozaki, T. & Raz, A. (1996). *Cancer Res.* **56**, 2960–2963.
Xu, W., Seiter, K., Feldman, E., Ahmed, T. & Chiao, J. W. (1996). *Blood*, **87**, 4502–4506.
Yakirevich, E. & Naot, Y. (2000). *Biol. Reprod.* **62**, 1016–1023.